



## Emergence of size induced metallic state in the ferromagnetic insulating $\text{Pr}_{0.8}\text{Sr}_{0.2}\text{MnO}_3$ manganite: Breaking of surface polarons

Proloy T. Das<sup>1</sup>, A. K. Nigam<sup>2</sup>, and T. K. Nath<sup>1</sup>

<sup>1</sup>Department of Physics, Indian Institute of Technology Kharagpur,  
Kharagpur - 721302, India.

dasproloy@phy.iitkgp.ernet.in; tnath@phy.iitkgp.ernet.in

<sup>2</sup>Department of Condensed Matter Physics and Material Science, Tata Institute of Fundamental Research,  
Homi Bhabha Road, Mumbai- 400005, India.

### ABSTRACT

Nano-dimensional effects on electronic-, magneto-transport properties of granular ferromagnetic insulating (FMI)  $\text{Pr}_{0.8}\text{Sr}_{0.2}\text{MnO}_3$  (PSMO) manganite (down to 40 nm) have been investigated in details. From the electronic and magnetic transport properties, a metallic state has been observed in grain size modulation by suppressing the ferromagnetic insulating state of PSMO bulk system. A distinct metal-insulator transition (MIT) temperature around 150 K has been observed in all nanometric samples. The observed insulator to metallic transition with size reduction can be explained with surface polaron breaking model, originates due to enhanced grain surface disorder. This proposed phenomenological polaronic model plays a significant role to understand the polaronic destabilization process on the grain surface regime of these phase separated nano-manganite systems. Temperature dependent resistivity and magnetoresistance data in presence of external magnetic fields are investigated in details with various compatible models.

### Keywords

Manganite nanoparticles, Magnetoresistance, Spin polaron hopping, Variable range hopping.

### Pacs

72.25.Dc, 73.63. Bd, 75.47.Lx, 75.75.Fk,



## Council for Innovative Research

Peer Review Research Publishing System

Journal: JOURNAL OF ADVANCES IN PHYSICS

Vol.8, No.2

[www.cirjap.com](http://www.cirjap.com), [japeditor@gmail.com](mailto:japeditor@gmail.com)

## 1.0 INTRODUCTION

Fascinating behavior in physical and magnetic properties of phase separated perovskite manganites turned on a new horizon in the field of condensed matter research from the last few decades [1]. The hole doped CMR manganites with general formula  $\text{Re}_x\text{R}_{1-x}\text{MnO}_3$ , where Re is trivalent rare earth ions (e.g. La, Nd, Pr, Sm) and R is divalent alkaline earth ions (e.g. Sr, Ca, Ba), are strongly correlated electron system where spin, charge, orbital and lattice degrees of freedom play very important role in their transport and magnetic behavior [2]. It is proposed that the CMR behavior could be well understood in the light of the double-exchange (DE) model [3] with a strong electron-phonon interaction [4-6]; however understanding of FMI state in under doped regime of manganite with the concept of DE mechanism is almost impossible. A strong electron-phonon coupling with the localized polaron in crystal lattice is believed to make the system insulating in nature [7], under such localization, the transport of electrons becomes predominantly phonon assisted. In earlier, it has been tried to give a satisfactory explanation with various kind of models like small polaron hopping (SPH) [8-10], variable range hopping (VRH) [11-13] etc. to understand these manganite system in details. It is also reported that a large MR as well as a large nonlinear electro-resistance can be observed in the FMI state of the underdoped bulk manganites [18]. For most of the half doped charge ordered insulating manganites where reduction of grain size renders the system metallic due to the destabilization of the charge ordering phenomena. There have been many works on optimally doped  $[\text{Pr}_{1-x}\text{Sr}_x\text{MnO}_3$  ( $0.3 \leq x \leq 0.6$ )] or on the half doped charge ordered manganites, however a few works have been reported so far in the case of under doped PSMO system [14-17]. We have addressed in this paper the interesting issue of grain size effect on FMI nature of PSMO bulk manganite. To the best of our knowledge, a detailed study of the effect of size reduction of PSMO manganites has not been carried out in details so far. We here report the nanometric size effects on the electronic- and magneto-transport properties of underdoped PSMO nanometric samples which have been analyzed with different suitable models. However, the most fascinating observation of this study is that the FMI state is destabilized and a ferromagnetic metallic state emerges with grain size reduction.

## 2.0 EXPERIMENTAL DETAILS

All the nanometric granular polycrystalline PSMO samples were synthesized by chemical pyrophoric reaction process [19]. We have employed aqueous solution of high purity  $\text{Pr}_6\text{O}_{11}$ ,  $\text{Sr}(\text{NO}_3)_2$ , and  $\text{Mn}(\text{CH}_3\text{COO})_2 \cdot 4\text{H}_2\text{O}$  taking in stoichiometric proportions. Tri-ethanolamine (TEA) has been added to the solution. After heating this complex solution at  $180^\circ\text{C}$  ash like black fluffy powder is obtained. After grinding this ash like fluffy powder for several hours, we have calcined it at four different temperatures ( $850^\circ\text{C}$ ,  $950^\circ\text{C}$ ,  $1050^\circ\text{C}$  and  $1250^\circ\text{C}$ ) to make the series of PSMO sample with different particle size.

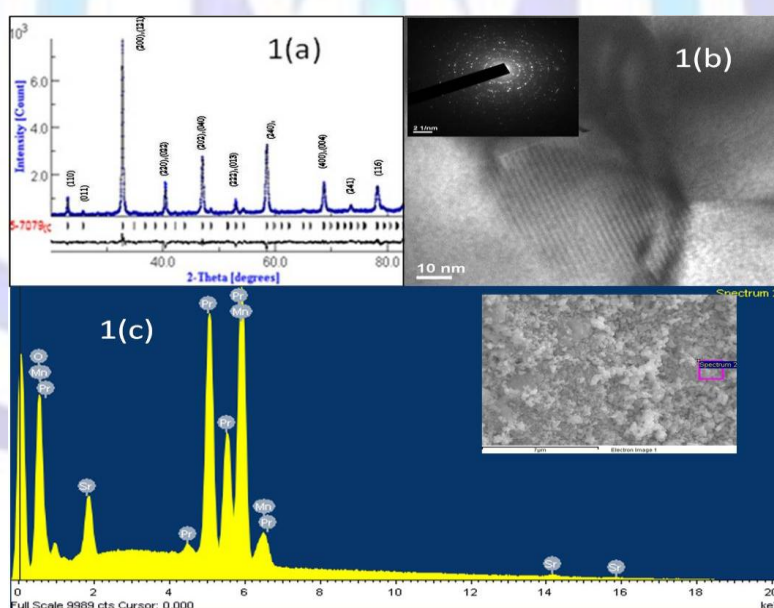


**Figure 1 (color online): (a) Rietveld refinement of HRXRD PSMO 950 sample, (b) and (inset) depicts lattice fringe in high resolution TEM micrograph and SAED pattern of PSMO 950 sample respectively, (c) EDS spectra and selected FESEM image of PSMO 950 sample with chemical stoichiometry.**

The crystallographic phase and crystalline nature analysis have been carried out through Rietveld refinement analysis of recorded XRD pattern. Single phase stoichiometry of PSMO samples have been analyzed using X-ray fluorescence spectroscopy (XRF) method. Field emission scanning electron microscopy (FESEM) images using microscope have been recorded Carl Zeiss SMT Ltd SUPRA™ 40 to observe the surface morphology of the nanometric grains of each samples. HRTEM micrographs have also been recorded for lowest particle size PSMO sample using JEOL 2010 electron microscope at an accelerating voltage of 200 kV. Selected area electron diffraction pattern (SAED) has been recorded to confirm the poly-/ single crystalline nature of the sample using the same instrument. Dc magnetization, temperature dependent Resistivity, MR measurements down to 4 K of these PSMO samples have been carried out under presence



of external high magnetic field and low temperature facilities: (a) 9 Tesla CFM VTI system and (b) SQUID magnetometer (Quantum Design, U.S.A). Complex ac-magnetic susceptibility measurements have been performed by a homemade susceptometer set up using a DSP Lock-in-amplifier (SRS-830, USA.) and a high precision temperature controller (Model-331, Lakeshore, USA). The set up has been calibrated by a standard low moment sample in the temperature range of 77-300 K.

### 3.0 RESULTS AND DISCUSSIONS

The microstructural properties of all PSMO samples are shown in Fig. 1 (a-c) respectively. Rietveld refinement of high resolution XRD data of all PSMO samples confirm the polycrystalline nature and single-phase orthorhombic structure with Pbnm space group as shown in Fig. 1 (a). Using Debye-Scherrer formula ( $\Phi = 0.9 \lambda / \beta_{\text{eff}} \cos \theta$ ), the average crystallite size of the PSMO samples have been estimated as ~ 40, 50, 58 nm and 0.2 micron with the sample sintering temperatures 850, 950, 1050 and 1250 °C, respectively [20].

**Table 1: Different crystallographic parameters estimated from Rietveld refinement (Column 2-6: lattice parameters c, a, b, unit cell volume, micro-strains). Magnetic fields, resistivity (with errors), activation energy (W) and density of states at the Fermi level (with errors) of various PSMO samples (Column 7-10)**

Sample PSMO	c (Å)	a (Å)	b (Å)	Volume (Å) <sup>3</sup>	micro-strain (x10 <sup>-4</sup> )	B (Tesla)	$\rho_0$ (x10 <sup>-4</sup> Ω-cm K <sup>-1</sup> )	Activation energy(W) (meV)	N(E <sub>F</sub> ) (x10 <sup>19</sup> eV <sup>-1</sup> cm <sup>-3</sup> )
850	5.4588	5.464	7.713	230.06	16.024	0	---	175.02	3.50(±0.001)
		2				5	160.59		
		9				9	146.42		
950	5.4613	5.471	7.713	230.51	9.6449	0	---	152.32	2.85 (±0.01)
		9	5						
1050	5.4654	5.474	7.726	231.19	8.1273	0	---	92.32	5.32 (±0.01)
		6	6						
1250 (bulk)	5.4789	5.474	7.738	232.13	9.6160	0	538.8 (±0.42) (80 K to 90K)	87.6	---
								134.98	
							1.8 (±0.47) (110K to140 K)	163.75	
							0.2 (±0.01) (175 K to 320 K)		
						5	223.3(±0.3) (79K to100 K)	87.01	
							4.8(±0.2) (105K to150 K)	120.23	
							0.4(±0.05) (200K to320 K)	157.47	
9	158.2 (±0.3) (80 K to 95K)	85.89							
	4.8(±0.2) (110K to150 K)	116.62							
	0.4 (±0.01) (175 K to 320 K)	151.68							

In Table 1 (column 2-6), we have summarized various microstructural parameters obtained from Rietveld refinement fitting of high resolution XRD pattern of the PSMO samples. No significant variation of lattice parameters in grain size modulation have been observed. The HRTEM lattice fringe of PSMO 950 (figure 1(b)) and the SAED pattern (inset figure 1(b)) reveal the polycrystalline nature and good crystallinity of the PSMO 950 sample, respectively. From the FESEM images of PSMO 850, 950, 1050 samples, it has been found that the grain size of the samples are nearly in hundred nanometers range whereas the grain size of PSMO 1250 sample is in micrometer-order (which are not shown here) and is expected to have bulk-like properties. In Fig. 1(c), the calculated chemical composition from the EDS spectra and recorded micrograph of the PSMO 950 sample has been depicted and corroborate the stoichiometry of our samples to a considerable limit. It is reported that distorted grain boundary and volume compaction of the unit cell in nanomanganite may induce strain and modify the crystal structure [21, 22]. However, in the studied PSMO system nominal change in volume and micro strain values are given in Table 1.

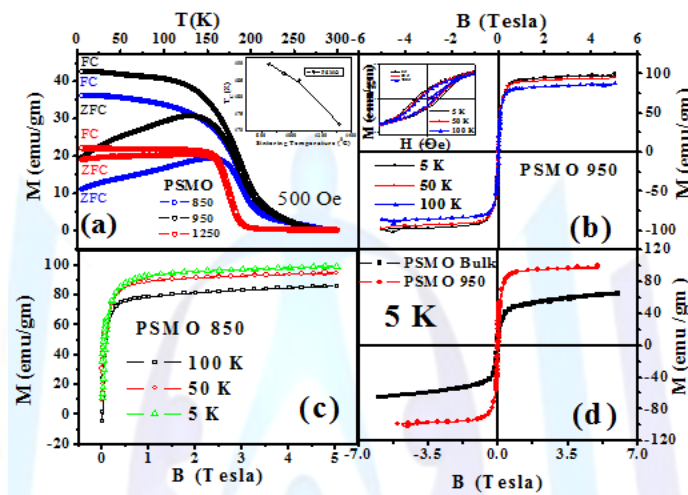


Figure 2 (color online): (a)  $M(T)$  of PSMO 850, PSMO 950 and PSMO bulk samples.; inset shows size induced  $T_c$  variation; (b)  $M(H)$  of PSMO 950 sample at 5 K, 50 K and 100 K respectively; (c) Saturation magnetization plot  $M_s(T)$  of PSMO 850 sample at 5 K, 50 K, and 100 K; (d) Comparison of  $M(H)$  study at 5K of PSMO 950 and PSMO Bulk samples

Dc SQUID magnetization study of all nanometric samples in the temperature range of 5-300 K at 500 Oe, are shown in Fig. 2(a) and the inset of the Fig. 2(a) depicts variation of  $T_c$  with grain size modulation. The calculated FC magnetization value of PSMO 850 sample at the lowest temperature is 48 emu/ gm. Ferromagnetic hysteresis behavior of PSMO 950 sample at 5, 50, and 100 K are depicted in Fig. 2(b). Virgin  $M(H)$  curves (only the first cycle) of PSMO850 sample at 5, 50 and 100 K are shown in Fig. 2(c) which reveals almost same saturation magnetization value at all measured temperatures. Similar nature has also been found for other two nanometric samples however, a drastic change in saturation magnetization value and emergence of FMM state from FMI state with size reduction has been revealed from a comparative  $M-H$  behavior of PSMO 950 and PSMO bulk sample as shown in Fig. 2(d) is already discussed elsewhere [19]. The complex ac-susceptibility for all samples with various temperatures and at a particular frequency 999.5 Hz is plotted in Fig. 3 for confirmation of ferromagnetic to paramagnetic transition temperature. It has been observed that in nanometric regime, the transition temperature  $T_c$  varies between 150- 185 K however, in the bulk system  $T_c$  is comparatively lesser than nanometric samples, same is reported by Rama et al. [23].

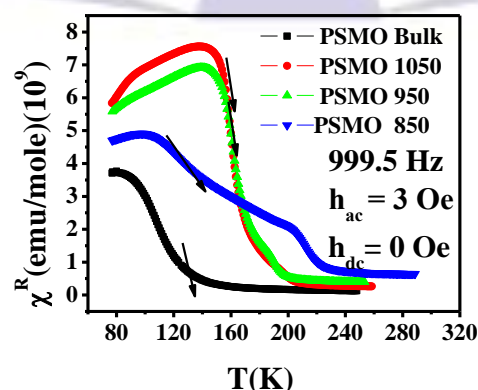
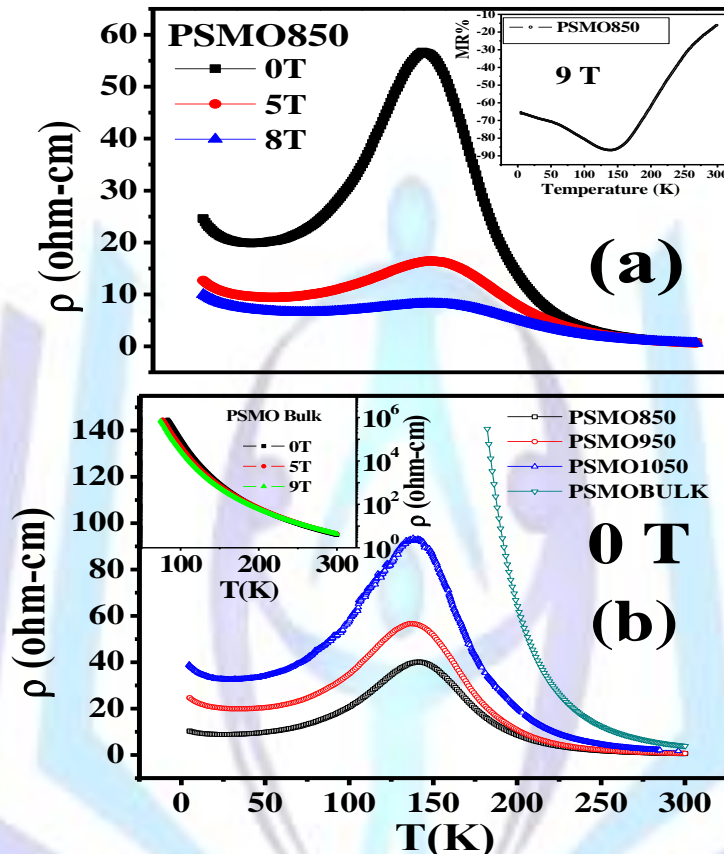


Figure 3 (color online): Magnetic ac-susceptibility plot with temperature of sample PSMO for different particle sizes.  $D = 40$  nm (PSMO 850).  $D = 50$  nm (PSMO 950). and  $D = 58$  nm (PSMO 1050).

### 3.1 Electronic transport

Temperature dependent resistivity of PSMO 850 sample under various external magnetic fields is plotted in Fig. 4 (a). It is found that with tuning the magnetic field, the resistivity peak of PSMO 850 sample is being suppressed. Figure 4(b) depicts the temperature-dependent resistivity behaviour of all PSMO samples where a drastic change of resistivity  $\rho$ , insulating ( $\sim 10^6 \Omega\text{-cm}$ ; inset of Fig. 4(b)) to metallic like state ( $\sim 16 \Omega\text{-cm}$ ) has been observed in grain size modulation which is also observed in doped manganite system [24, 25]. No systematic variation in stoichiometry with sintering temperature has been found in any of the measured sample which is verified through EDS, XRF, and chemical titration procedures. This kind of colossal change in resistivity of the present system is most implausible due to variation of stoichiometry, originates from sintering temperature. Therefore we believe that this unusual behavior of resistivity finds a correlation between grain size and surface disorder, which suppress the FMI state and evolve the FMM state with size reduction.



**Figure 4 (color online): (a) Resistivity as a function of temperature of PSMO 850, sample at different magnetic fields 0 T, 5 T and 9 T; In the inset of Figure (a) depicts MR% variation with temperature of PSMO 850 sample at 9 Tesla magnetic field (b) Resistivity plot with temperature for four different particle sizes at 9 T; In the inset of (b) shows resistivity as a function of temperature of PSMO 1250 (bulk) sample.**

From the inset of Fig. 4(a), we have found that MR minima appears around 160 K for PSMO 850 sample which is very closely to  $T_p$ , corroborate the CMR effect in the underdoped manganite system. Formation of FMI state in this manganite system can be explained using orbital polaronic lattice model which proposed by Geck J et al. [26, 27]. This model includes orbital reordering and strong existence of orbital-hole coupling to clarify the CMR type behavior near MIT temperature. In this kind of underdoped Pr-Sr-Mn-O system, local Double exchange (DE) mechanism may help to stabilize the bulk FMI state, which usually appears due to formation of polarons.

in the context, it is also noticeable that there are no significant changes in lattice parameters as well as in crystalline volume in nanometric grain size modulation as shown in Table 1. To find out the pressure effect on unit cell volume in the present PSMO system, the measured data was fitted with Birch-Murnaghan model [28, 29] which can be written as,

$$P = \frac{3}{2} B_0 (x^{\frac{7}{3}} - x^{\frac{5}{3}}) [1 + \frac{3}{4} (B' - 4)(x^{\frac{2}{3}} - 1)] \dots \dots \dots (1)$$

where,  $x = V/V_0$  is the relative volume change,  $V_0$  is the unit cell volume at  $P=0$ ,  $B_0$  and  $B'$  are the bulk modulus [ $B_0 = -V(dP/dV)_T$ ] and its pressure derivative [ $B' = (dB_0/dP)_T$ ]. This equation has a correlation between changes in unit cell volume to calculate the pressure. Employing the above equation the extracted pressure values for PSMO 850, 950 and 1050 nanometric samples are 0.049 GPa, 0.176 GPa, and 0.088 GPa respectively considering the value of  $B_0 = 225(5)$  GPa with fixed  $B' = 4$  for  $\text{Pr}_{0.52}\text{Sr}_{0.48}\text{MnO}_3$  system as reported by Kozlenko et al. [29]. Calculated pressure values from the above equation reveals that there is almost no pressure effect on nanometric samples coming from surface tension

however, the result shows a contrasting behavior between the nanometric grains and its bulk counterpart and can be explained using enhanced surface disorder model [30]. Henceforth, to find out the origin of FMI and FMM state which arises in the present under doped PSMO system with size reduction, we have proposed a phenomenological surface polaron model. We believe that this model will be helpful to understand the physical mechanism of this unusual resistive state which arises in with size reduction in these strongly correlated systems. Destabilization of FMI state at the surface grain boundary is primarily attributed to the surface reconstruction of the electronic states with size reduction of PSMO samples and increases possibility of DE mechanism inside the system. Enhanced surface to volume ratio in nanometric grains adds up to the sizeable change in electronic transport (metallicity), enhanced magneto-transport and magnetic properties and indicates the collapse of polaronic order at the grain surface of nanometric samples, can be explained by a phenomenological core shell model as shown in Fig. 5 by four segments. In the Fig.5 (1), formation of FMI state between grains due to carrier localization is shown by dark green color. It is very difficult to distinguish any surface and the core of the grains in this regime due to homogeneous distribution of localized carriers. Destabilization of surface disorder in nanometric regime is depicted in Fig. 5 (2), and 5 (3), respectively by showing the diffusion of dark green color in light yellow color matrix. Light yellow color indicates the surface disorderness, and induces the ferromagnetic metallic property in nanometric regime, however, in both cases, the core of the grains shows FMI behavior. Any kind of crystal defects or surface disorder cannot affect on the core polarons and makes the possibility of coexistence of FMI and FMM state. Most probable inter grain hopping of electrons through a low resistive path, as a consequence of small polaron breaking on outer surface of the nanometric grains is shown in Fig. 5 (4). On the other hand, any kind of crystalline defects and presence of surface disorder increases the probability of enhancement of surface to volume ration, which is very much relevant with nanometric samples. As a result, destabilization of polaron occurs predominantly on the surface of the nanometric grains and itinerant electrons start the conduction mechanism between inters grains to make the system a ferromagnetic metal.

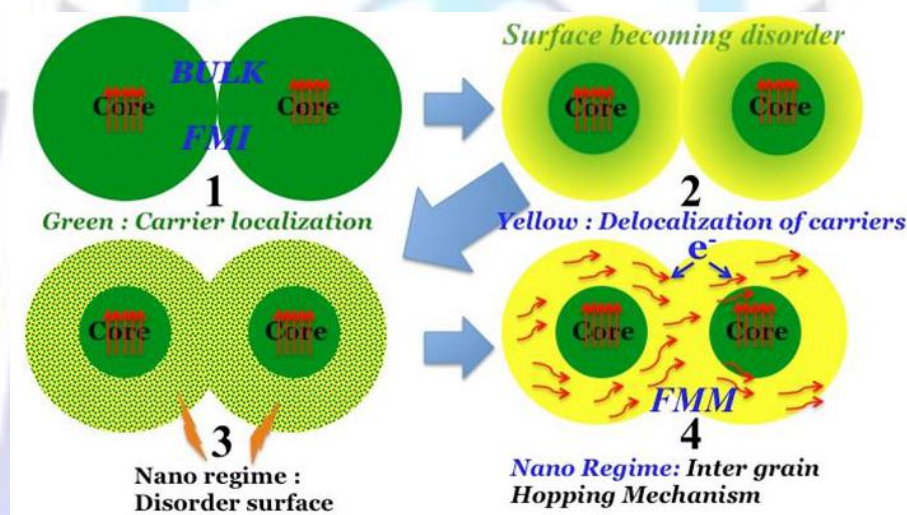


**Figure 5 (color online): Schematic representation of the phenomenological model: Breaking of surface polarons. Color code: Dark green (strong carrier localization; appears of FMI state) to light yellow (surface disorder and carrier destabilization; FMM state).**

A detailed analysis of measured resistivity data has also been made employing different suitable models to underlying electronic transport mechanism of the Pr-Sr-Mn-O system. Firstly, we have used small polaron hopping (SPH) model considering non adiabatic approximation [9, 10] which can be written as,

$$\rho = \rho_0 T \exp\left(\frac{W}{k_B T}\right) \dots \dots \dots (2)$$

where, T, W and  $\rho_0$  stands for absolute temperature, activation energy and pre-exponential factor which has the form of  $[k_B / u_{ph} N e^2 R^2 C (1-C)] \exp(2\alpha R)$ , Here  $k_B$  is Boltzmann constant,  $u_{ph}$  is the optical phonon frequency, N is the number of transition metal ions per unit volume, R is the average hopping distance, C is the fractional occupancy of the polarons and  $\alpha$  is the tunneling probability of the electronic wave function decay constant, respectively. It fits very well with the experimental data of bulk system. To justify our SPH model we have calculated the polaronic radius ( $r_p$ ) which has the form of  $(1/2) [\pi/6N]^{1/3}$  and found that it lies within 1.37 to 1.40 Å for PSMO samples. This is much smaller than one unit cell volume and indicates the applicability of our model. It is clear that, small area of a unit cell can be localized by these small polarons. Figure 6(a) shows the SPH fitted graphs at different magnetic fields of PSMO Bulk system as well as for PSMO 850 nanometric sample (in the inset of Fig. 6(a)). Pre-exponential factor ( $\rho_0$ ), can be calculate from the slope of the plotted  $\ln(\rho/T)$  vs  $1/T$  graph. The various fitting parameters which have been extracted using Eqn. (4) are summarized in Table 1. It is observed that the resistivity data, cannot be fitted with this equation in the whole temperature regime due to change of slopes at different temperature scale. Therefore we have sorted out selective temperature regimes and fitted with Eqn. (2) which provides higher value of  $\rho_0$  at low temperature regime compare to other regime. At low temperature regime,  $\rho_0$  values increases mainly due to charge localization and may be due to enhanced magnetic surface disorder. In

low temperature regime, the parameter,  $\alpha$  varies whereas other parameters are almost constant. According to SPH model, activation energy is not responsible for the higher value of resistivity at low temperature regime as its shows a decreasing nature. We have investigated the dependency of activation energy with tuning of magnetic field and obtained values are tabulated in Table-1. Monotonically decreasing nature of activation energy with increasing of magnetic fields (up to 9 T) can be attributed to the delocalization of polarons in phase separated regime of this strongly correlated electron systems. Interestingly, activation energy is higher in lowest nanometric sample (PSMO 850) compared to other two (PSMO950 and PSMO1050), similar nature of activation energy has been observed by Kundu et al. for NSMO nanometric samples [10]. We have also investigated the effect of magnetic field on activation energy at nanometric regime as furnished in Table 1. In the paramagnetic regime, the zero field resistivity data of all nanometric samples have been fitted according to Mott's variable-range-hopping (VRH) model which can be written as,

$$\ln\left[\frac{\rho}{\rho_{\infty}}\right] = \left[\frac{T_0}{T}\right]^4 \dots\dots\dots(3)$$

The best fitted resistivity data employing eqn. 3 in the paramagnetic regime of PSMO nanomanganites are shown in Fig. 6 (b). The VRH model [11] was originated to explain the electronic conduction process of doped semiconductors. Insight picture of VRH model is that, electrons bears a hydrogenic orbital with a wave function  $\psi = \psi_0 \exp(-\alpha r)$  and has become localized by the potential fluctuation of dopants.

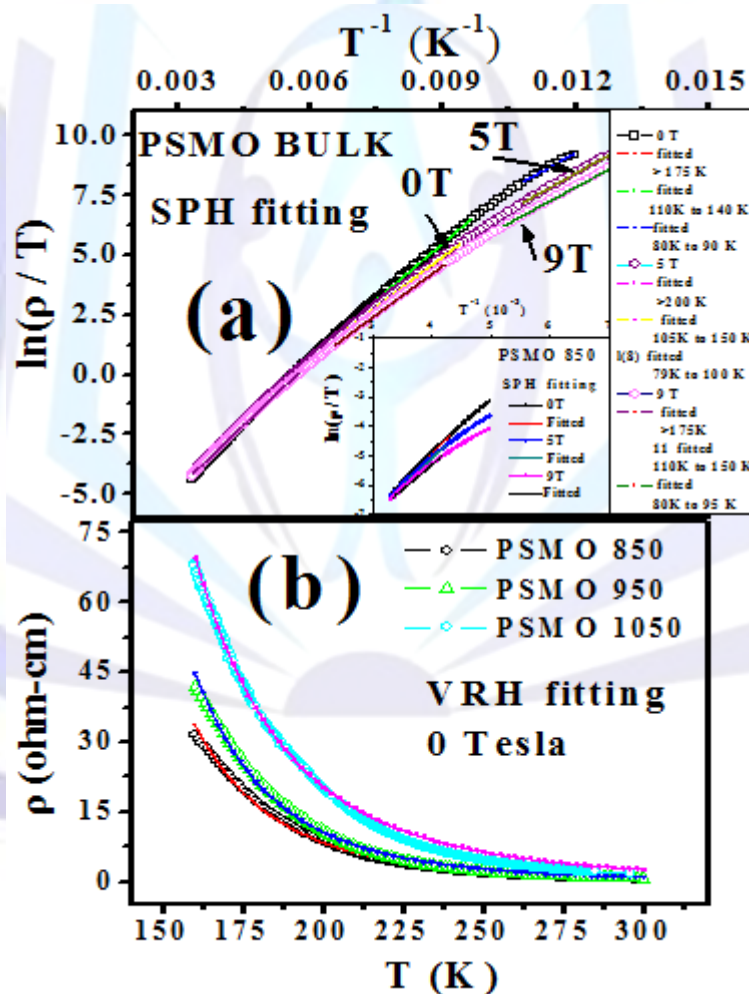


**Figure 6 (color online): (a) SPH fitting of PSMO Bulk sample at different slopes for different magnetic fields; In the inset of (a) shows SPH fitting of PSMO850 sample at different magnetic fields; (b) VRH fitting of PSMO950, PSMO950, PSMO1050 samples under without field.**

The hopping mechanism of electrons can be conducted due to the competitive behavior of potential fluctuation and the site distance (R) of electrons. The hopping rate at a particular site R and at a given energy value  $\Delta E$  is given by,

$$\gamma = \gamma_0 e^{[-2\alpha r - \Delta E/k_B T]} \dots\dots\dots(4)$$

Hopping rate can be minimized using the lowest value of  $\Delta E [ = 4/3\pi R^3 N(E) ]^{-1}$  and  $R \{ = (9/[8\pi\alpha N(E) k_B T])^{1/4} \}$  and takes the final expression of resistivity (Mott expression),

$$\rho = \rho_{\infty} e^{2.06 \left[ \frac{\alpha^3}{N(E) k_B T} \right]^{1/4}} \dots\dots\dots(5)$$

The detailed numerical calculations have reported earlier by Viret et al. [12]. We have calculated the approximate density of available states of carriers at the Fermi level employing the equation,

$$k_B T_0 = \frac{18\alpha^3}{N(E)} \dots\dots\dots(6)$$

The extracted parameters are furnished in Table 1. Assuming the value of  $\alpha$  as  $2.22 \text{ nm}^{-1}$ , it is observed that  $N(E)$  value is  $\sim 10^{19} \text{ eV}^{-1} \text{ cm}^{-3}$  which is reasonable compare to other manganites system [13]. Considering the extracted fitting parameters and  $R^2$  values of both SPH and VRH models, it can be concluded that VRH model fits better in nanometric regime.

### 3.2 Magneto- transport

Colossal magneto resistance (CMR) effect is related to the intrinsic properties of optimally doped manganites, occurs near the magnetic phase transition temperature  $T_C$ . The CMR effect in single crystal is mainly due to enhancement of transfer integral  $t_{ij}$  via suppression of the spin fluctuation by the applied magnetic field ( $MR_{INT}$ ). High magnetic field is necessary to align the spin and shows maximum MR near  $T_C$ . For the polycrystalline sample another contribution in MR also arises due to the spin polarized tunneling (SPT) across the ferromagnetic grains at low magnetic field (LFMR).

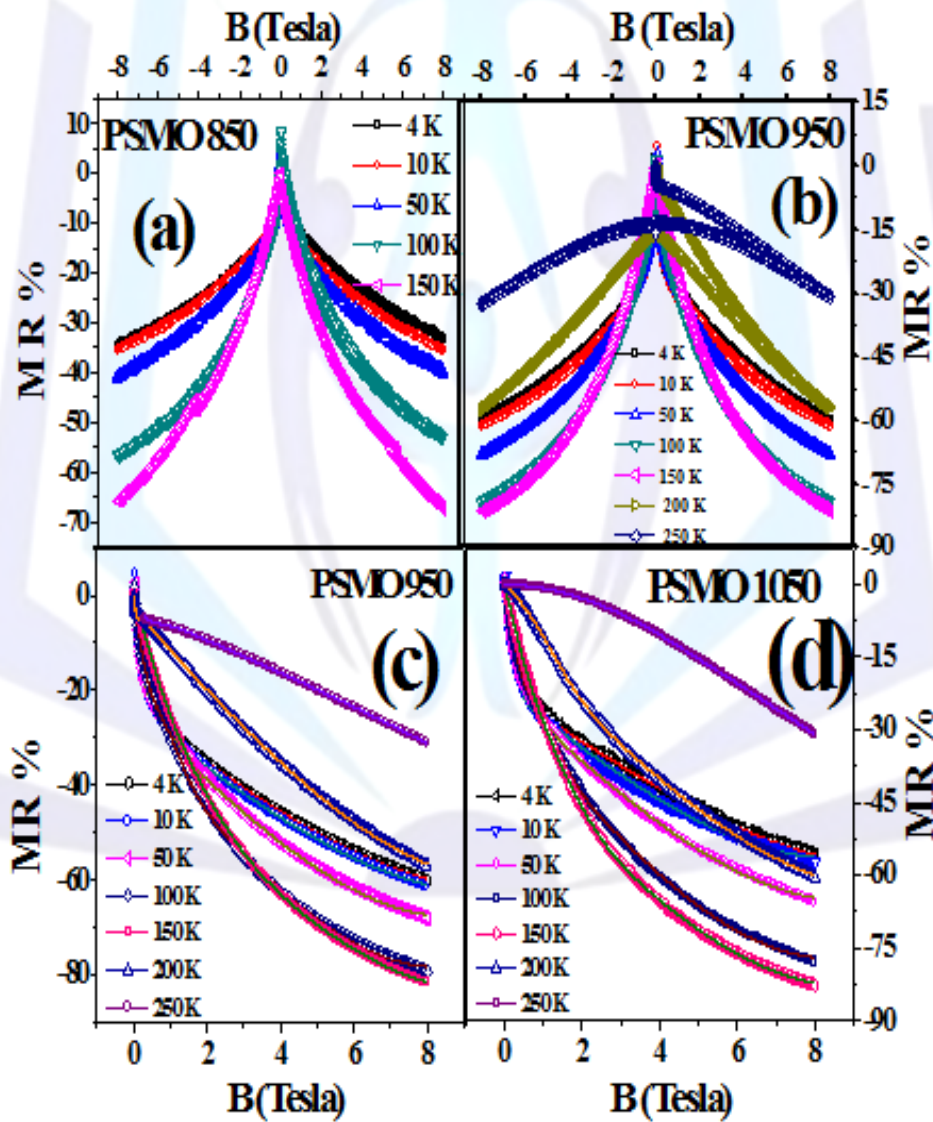


Figure 7 (color online): (a-b) HFMR behavior of PSMO 850, 950 samples respectively; (c-d) shows MR graphs of PSMO 1050 and 950 samples fits well with the proposed model of Raychoudhuri et al.



**Table 2: Spin polarized tunneling and intrinsic contributions of MR for all nano-metric PSMO samples of different particle size at various temperatures and magnetic fields.**

Sample PSMO	B (Tesla)	4 K		10 K		50 K		100 K		150 K	
		SPT	INT	SPT	INT	SPT	INT	SPT	INT	SPT	INT
850	1	10.5 7	3.41	10.04	3.79	10.44	~4.73	9.47	~8.1 5	13.38	~6.22
950	1	22.5 1	5.35	23.09	~5.76	21.27	~6.87	20.39	~8.8 8	16.80	8.02
1050	1	21.5 9	5.17	21.63	~6.15	20.64	~7.17	18.78	~9.0 1	20.40	8.18

Figure 7(a-b) shows the field dependent MR ( $MR\% = ([\rho(H) - \rho(0)] / \rho(0)) \times 100$ ) at different temperatures of PSMO850 and PSMO950 samples. It is observed that CMR reaches a maximum value (-85% ~ -90%) near  $T_p$  and then decreases gradually with the increase of temperature. Maximum MR near  $T_p$  indicates the instability and phase separation behavior of the PSMO sample. At lowest temperature (4K) the maximum MR is ~ 85% for the sample at a field of 8 T for 40 nm (PSMO 850) particle size. For the bulk sample the MR is ~ 50% at 150 K at 8T magnetic field. Details investigations of CMR behavior of PSMO samples have been carried out with the variation of temperature as well as magnetic field. To separate out the contributions of spin polarized tunneling ( $MR_{SPT}$ ) and intrinsic MR ( $MR = MR_{SPT} + MR_{INT}$ ) part in measured MR value for the PSMO system, a proposed model of Raychoudhuri *et al.* has been used [31] which can be expressed as,

$$MR = -\int_0^H [A \exp(-Bk^2) + Ck^2 \exp(-Dk^2)] dk ("MR_{SPT}") - JH - KH^3 ("MR_{INT}") \dots \dots \dots (7)$$

where,  $k$  is the pinning strength which is distributed over grain boundary and the rest adjustable fitting parameters A, B, C, D, J and K are evaluated from a nonlinear least-square fitting. Applicability of this SPT model associated with intrinsic contribution of MR for all PSMO nanometric samples have been justified with the consideration of the pinning of domains at the grain boundary and enhancement of grain surfaces. The entire fitted curves employing the above equations are shown in Fig. 7(c) and 7(d) for PSMO 950 and PSMO 1050 nanometric samples respectively. From the fitted curves of PSMO 850 (not shown here), PSMO 950, PSMO 1050 samples, the spin polarized tunneling MR contribution as well as the intrinsic MR contribution in net magneto resistance have been calculated which are summarized in Table 2. This phenomenological model signifies that, SPT of carriers are more effective in low field regime between highly spin-polarized grains due to inter granular tunneling of carriers where as intrinsic (INT) DE mechanism plays a dominant role at high field regime in intra-grain region. A detailed analysis of SPT and INT contributions for our PSMO nanometric samples in lower magnetic field (~1 T) are tabulated in Table-2. The value of both  $MR_{SPT}$  (~25-30%) and  $MR_{INT}$  (~ 44 – 48%) increases with the increasing of temperature from 5 K to 150 K at different magnetic fields. At low field  $MR_{SPT}$  contributions dominant as compared to  $MR_{INT}$  contribution and for lowest particle size PSMO 850, it shows a minimal value (~10.5%) compare to other two samples PSMO 950 ( $MR_{SPT}$  ~23%) and PSMO 1050 ( $MR_{SPT}$  ~22%) samples.

**4.0 CONCLUSIONS**

In summary, a detailed investigations has been carried out on magneto-, and electronic transport properties of  $Pr_{0.8}Sr_{0.2}MnO_3$  system in grain size modulation. Appearance of FM metallic state in nano regime compared to its FM insulating bulk counter part has been explained as destabilization of surface polaronic transport due to the enhanced surface disorder at the grain surface and it opens a low resistive conduction path between neighbor ferromagnetic domains by enhancing the probability of DE mechanism in nanometric dimension. The insulating and metallic part of the resistivity data in presence of external magnetic fields have been fitted with conventional models. In observed CMR effect SPT (electron tunneling across ferromagnetic grains (inter granular)) contribution and intrinsic contribution of each grain have also been calculated. It is found that in low temperature regime, spin ploarization tunneling contribution is more compare to intrinsic contribution. These fascinating outcomes in resistivity and presence of CMR effect of these PSMO nanometric samples may have a good potential application in magnetic memory chip and magneto resistive device fabrication.

**ACKNOWLEDGMENTS**

Authors are thankful for financial support from different funding agencies: (a) DAE (BRNS) through project S.L. No. 2006/37/52/BRNS/2376, dated 16.01.2007, (b) CSIR through Award no.: 09/081 (1077)/ 2010-EMR-I to carry out this research work. PTD is thankful to the Central Research Facility, IIT Kharagpur for various experimental facilities. PTD also thank to D.K. Pradhan, University of Puerto Rico, U.S.A. for performing the XRF measurement.



## REFERENCES

- [1] Tokura Y, *Colossal Magneto resistive Oxides*, Gordon and Breach Science, Singapore, (2000).
- [2] Dagotto E, Hotta T, Moreo A, *Physics Reports* 344 (2001); Dagotto E, *Science*, 257 (2005).
- [3] Zener C, *Phys. Rev.* 82, 403 (1951).
- [4] Roder H, Zang Jun, and Bishop A R, *Phys. Rev. Lett.* **76**, 1356 (1996).
- [5] Mills A J, Shraiman Boris I, and Mueller R, *ibid*, **77**, 175 (1996).
- [6] Lee J D and Min B I, *Phys. Rev. B* **55**, 12 454 (1997).
- [7] Mizokawa T, Khomskii D I, and Sawatzky G A, *Phys. Rev. B* **63**, 024403 (2000).
- [8] Schramm S, J Hoffmann and Ch Jooss, *J. Phys.: Condens. Matter* **20**, 395231(2008).
- [9] Mollah S, Khan Z A, Shukla D K, Arshad M, Kumar Ravi, and Das A, *J.Phys. Chem.Solids*, **69**, 1023 (2008).
- [10] Kundu S and Nath T K, *J. Phys.: Condens. Matter*, **22** 506002(2010).
- [11] Mott N F and Davies E A, *Electronic Processes in Noncrystalline Solids*, 2<sup>nd</sup> ed. –Oxford University of Process, New York, 1979 ; H. Boettger and V. Bryksin, *Hopping Conduction in solids*, Akademic -Verlag, Berlin, 1951.
- [12] Viret M, Ranno L, and Coey J M D, *Phys. Rev. B* **55**, 8067 (1996).
- [13] Banerjee A, Pal S, Rozenberg E, and Chaudhuri B K, *J. Phys.: Condens. Matter* **13**, 9489(2001).
- [14] J M Liu, Y. Yang, J. Li, T. Yu, Q. Huang, and Z. G Liu, *Presented at the 8 th international conference on Electronic Materials (IUMRS-ICEM, 2002 Xi'an, China,10-14 June (2002).*
- [15] Yang J, Lee Y P, and Li Y, *Phys. Rev. B* **76**, 054442 (2007).
- [16] Huang X H, Ding J F, Hou Y, Yao Y P and Li X G, *Phys. Rev. B* **78**, 224408 (2008).
- [17] Zhu X, *J. Magn. Magn. Mater*, **321**, 15 (2009).
- [18] Jain Himanshu, Raychaudhuri A K, Mukovskii Ya M, and Shulyatev D, *Appl. Phys. Lett.*, **89**, 152116 (2006).
- [19] Dey P, Nath T K, *Phys. Rev. B* **73**, 214425(2006)
- [20] Das P T, Taraphder A, Nath T K, AIP Conf. Proc. **1349**, 383 (2011)
- [21] Shantha K, Shankar Kar S, Subbanna G N and Raychaudhuri A K, *Solid State Commun.* **129**, 479 (2004).
- [22] Sarkar Tapati, Raychaudhuri A K, Bera A K, and Yusuf S M, *New J. Phys.* **12**, 123026 (2010).
- [23] Rama N, Sankaranarayanan V, Ramachandra Rao M S, *J. Appl. Phys.* **99**,08Q315 (2006).
- [24] Cheikh-Rouhu A, Koubaa M, Boujelben W, Cheikh-Rouhu Koubaa W, Haghiri- Gosnet A M, Renardm J P, *J. Magn. Mater*, 272-276, 432-433 (2004).
- [25] X C Martin, A. Maignan, M. Hervieu, and B. Raveau, *Phys. Rev. B* **60**, 12191 (1999).
- [26] Geck J, Wochner P, Kiele S, Klingeler R, Reutler P, Revcolevschi A, and Bu'chner B, *Phys. Rev. Lett.*, 95, 236401 (2005).
- [27] Geck J, Wochner P, Kiele S, Klingeler R, Revcolevschi, Zimmermann V M, Bu'chner, and B A Reutler P, *New J. Phys.*, 6, 152 (2004).
- [28] Kozlenko D P, Dubrovinsky L S, Goncharenko I N, Savenko B N, Voronin V I, Kiselev E A, and Proskurnina N V , *Phys. Rev. B* **75** 104408 (2007).
- [29] Kozlenko D P, Dubrovinsky L S, Jirak Z, Savenko B N, Martin C, and Vratislav S, *Phys. Rev. B* **76**, 094408 (2007).
- [30] Kundu S, Nath T K, Nigam A K, Maitra T, and Taraphder A, *arXiv : 1006.2943, [cond-mat.str-el]*, 15 Jun 2010.
- [31] Raychaudhuri P, Nath T K, Nigam A K, and Pinto R, *J. App. Phys.* **84**, 2048 (1998).